# Removing metal debris from thermosetting EMC powders by Nd-Fe-B permanent magnets

Yowching Liaw[1,a], Jung-Hua Chou[1] and Shouyen Chao[2]

[1]*Department of Engineering Science, National Cheng Kung University, Tainan, 70101, Taiwan*
[2]*Department of Electronic Engineering, Minghsin University of Science and Technology, Hsinchu, 30401, Taiwan*

**Abstract.** During the preparation of thermosetting encapsulation molding compounds (EMCs) for semiconductor packaging, metal debris are always present in the EMC powders due to the hard silica fillers in the compound. These metal debris in the EMC powders will cause circuit shortage and therefore have to be removed before molding. In this study, Nd-Fe-B permanent magnets are used to remove these debris. The results show that the metal debris can be removed effectively as the rate of accumulation of the metal debris increases as time proceeds in the removing operation. The removal effectiveness of the debris is affected by both the magnetic flux density and the flow around the magnet. The wake flow behind the magnet is a relatively low speed recirculation region which facilities the attraction of metal debris in the powders. Thus, the largest amount of the accumulated EMC powders occurs downstream of the magnet. Hence, this low speed recirculation region should be better utilized to enhance the removal efficiency of the metal debris.

## 1 Introduction

The electronic packaging industry plays the cap stone role in the semiconductor industry because it is the last step in the whole manufacturing process of making electronic components. Currently, these components are forced into the realm of higher input/output (I/O) counts due to the ever quest for electronic products with high performance and lower cost of consumers. Higher I/O counts imply the reduction of the I/O pitch of IC chips. The immediate consequence of this pitch reduction is that the tolerance of metal debris in the encapsulation molding compounds (EMCs) is extremely restricted in order to avoid short circuits. This type of short circuit is very different from that due to wire sweeping [1, 2] which can be resolved by proper wire bonding and molding. The short circuit caused by metal debris can only be resolved by removing them from the EMCs.

The metal debris in the molding compounds can originate from several sources such as metals in the raw materials or those generated during the manufacturing process [3]. The latter situation typically occurs because EMCs are thermosetting materials and presently silica is the most common EMC filler with a large weight percentage of approximately 75%. The hardness of silica of Mohs scale 7 is very large for the facilities used in making the compounds during blending, kneading, and transporting through the metal piping system. Thus, metal debris can be produced due to abrasion or erosion of the facilities and have to be removed for reliability requirement as described above.

Even though the removal of metal debris in the EMC powders is essential in the electronic packaging industry, the related issue was rarely reported in the literature. This situation is very unique comparing to other industries facing similar issues, such as those in making foods, drugs, general powders [4-8], and metal machining [9, 10]. For the food, drug, and general powder industries, the causes of metal debris are similar to those of EMCs. Whereas, for the metal machining industry, metal debris are a by-product. Hence, for these industries, various methods have been applied to remove metal debris. These methods of removal are generally based on permanent magnets as the debris are usually ferromagnetic materials [4-10]. However, comparing to these industries, the uniqueness of lacking in the literature of metal debris removal in the EMC industry deserves special attention. Thus, this study intends to fill in this gap by presenting a technique which can remove metal debris in the EMC powders effectively for industrial applications.

Typical metal debris generated in the production of EMCs as shown in Fig. 1 are of slender types, including ribbon, sheet, and bulk shapes. Because of different shapes, their weights are also very different. In reality, these debris are generally enclosed by the EMC powders and therefore need to be removed by proper solvant to obtain the metal

[a] Corresponding author: n9897121@mail.ncku.edu.tw

debris alone. In this study, the metal debris with the EMC powders are removed by magnets. Hence, in the following sections, design and implementation of the removing setup is presented first, followed by the removal experimental results and conclusions.

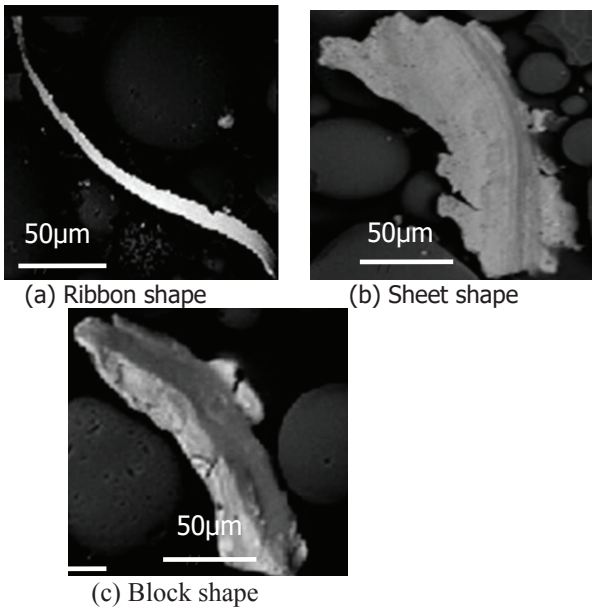


(a) Ribbon shape (b) Sheet shape

(c) Block shape

**Figure 1.** Typical shapes of metal debris in the EMC powders

## 2 Design and implementation of the Nd-Fe-B magnets

Due to energy considerations, the magnets adopted in removing metal debris are always of high strength permanent types, notably Nd-Fe-B magnets. In general, the geometry of the magnets is either flat or cylindrical. It is well known from fluid flow principles [11] that the form drag of a flat magnet is much larger than that of a cylindrical magnet. Moreover, the mesh type arrangement of the magnets tends to cause blockage [4, 7] because of aggregation due to the van der Waal force and accumulation of the powder particles to the magnets due to the magnetic force. Hence, the configuration of the parallel arrangement of magnets is selected in this study.

As the efficiency of separation of metal debris from EMC powders depends on the size, density and speed of the metal debris, and magnetic strength [8], a proper selection of the magnets and their arrangement are essential. Thus, the field strength of the proposed parallel configuration is examined first as follows.

### 2.1 Field strength of magnets versus distance

In order to determine the proper configuration of the magnets, the magnetic field strengths were measured first. Two types of magnets of different diameters of 134mm and 25mm, respectively were evaluated for their suitability. The magnets were formed by aligning the magnetic blocks with the same polarity inside a stainless shell of 1mm in thickness. The gap between the magnetic blocks chosen for this study was 5.5mm. The field strength in terms of magnetic flux density in Gauss was measured by a Gauss meter which was mounted on a height gauge. The magnet flux density was measured by varying the distance between the probe and the magnet surface. The measuring facility was setup on a granite platform as shown in Fig. 2.

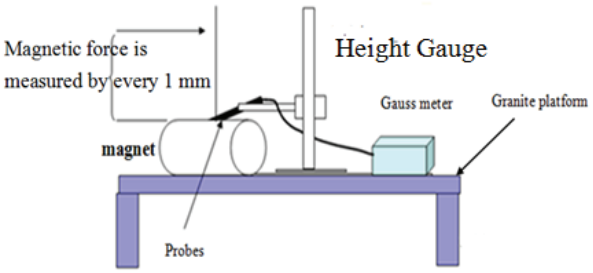


**Figure 2.** A schematic diagram of the magnetic field strength measurement facility

Fig. 3 depicts the magnetic field strengths of the two types of Nd-Fe-B permanents normalized by the field strength of the smaller magnet. In addition to the fact that the magnet flux densities of both magnets decrease as the distance between the Gauss meter and the surface of the magnet increases, the flux density of the magnet of 134mm in diameter is always larger than that of the 25mm magnet, irrespective of the distance from the surface of the individual magnet.

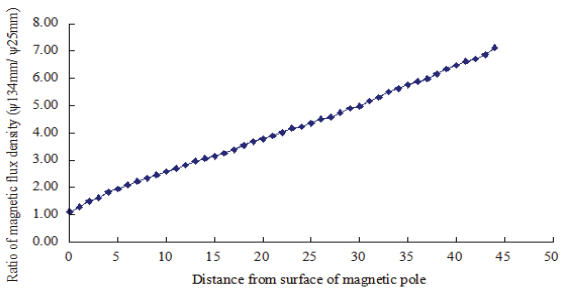


**Figure 3.** Normalized field strength versus distance from the surface of the magnet

Despite the fact that a higher magnetic flux density can be achieved by the larger magnet, the smaller magnet of 25mm in diameter was adopted in this study so that more magnets could be installed in a given space to generate a more uniform distribution of the magnetic flux density. Hence, the smaller magnet was selected in this study.

### 2.2 Field strength of magnets versus gap

For debris attraction, Nd-Fe-B magnetic blocks were arranged with the same polarity facing each other. Hence, the magnetic force is larger when the gap between the poles of the same polarity is smaller. To quantify this gap effect, a magnet with two magnetic blocks inside a SUS304 stainless tube with an inner diameter of 25mm was designed for this purpose. The gap between the poles was adjusted continuously so that the magnetic field intensity on the tube surface could be measured.

The results are portrayed in Fig. 4. For the gap between 0 and 40mm, two trends can be observed. One is that the

smaller the gap, the larger the flux density, consistent with the results of the literature [12-14]. The other is that the rate of decreasing of the magnetic flux density reduces as the gap increases. That is, the flux density reduces more rapidly for smaller gaps and then gradually levels off to a constant value as the gap reaches 20mm and beyond. Thus, for the present study, the gap of 5.5mm was selected.

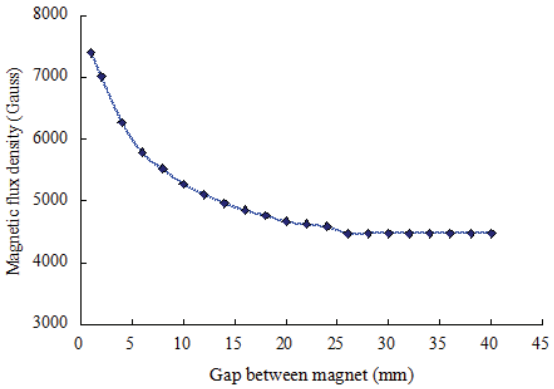


**Figure 4.** Surface Magnetic flux density versus pole gap

### 2.3 Facility for debris removal

The facility for removing the metal debris is drawn in Fig. 5. The facility consisted of a T-shaped upper hopper with a square cross-sectional area and a lower chamber with the magnets. The EMC powders were released from top of the hopper and moved through the hopper and the magnet chamber by free falling. The hopper was about 177mm in height with the entrance area of 350mm by 350mm and exit area of 255mm by 255mm. The magnet chamber housed five Nd-Fe-B magnets of 25mm in diameter and 208mm in length; the gap between the neighboring magnets was 32mm. Each magnet had seven Nd-Fe-B blocks with six gaps; the size of each gap was 5.5mm.

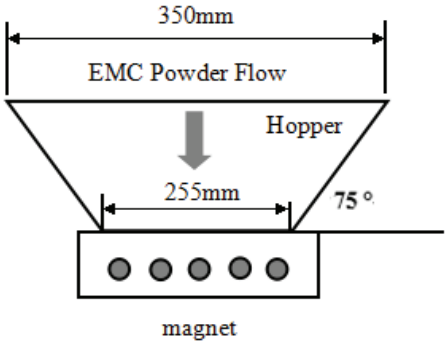


**Figure 5.** The facility for collecting EMC powders with metal debris

The EMC powder entered the hopper from the top at a mass flow rate of 1200kg/hr continuously for four hours. Afterwards, the magnets were removed from the magnet chamber to measure the thicknesses of the EMC powders attracted by the magnets. Since the shape of the EMC powders attached to the magnets was not circular due to the flow around the magnet, four dimensions, X1, X2, Y1 and Y2, as shown in Fig. 6 were used to quantify the attraction of the EMC powders. The symbol Y and X denote the gravitational direction and the direction perpendicular to gravity, respectively.

As the metal debris were covered by the EMC powders, the powders were removed from the magnets after thickness measurements. Then solvents were used to dissolve the EMC powders to separate the metal debris from the EMC powders. Then, the weight of the metal debris was measured afterwards.

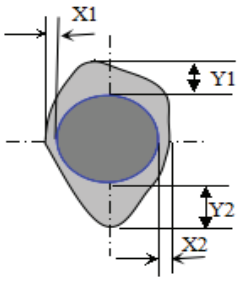


**Figure 6.** Measurement dimensions of EMC powders versus the magnet

## 3 Results and discussion

As described above, the magnets were removed from the magnet chamber to measure the thickness of the EMC powders attracted by the magnets after continuous operation for four hours. Typical shapes of the attached EMC powders are portrayed in Fig. 7 from the top view for visual observation. The numerals in the figures denote the numbers of the five magnets installed in the magnet chamber.

Two trends can be observed from the shape of these EMC powders on the magnets. One is that more powders were attracted by the two magnets at the two sides of the magnet chamber. This is due to the convergent geometry of the hoper to direct more EMC powders passing over the two magnets at the sides than those three in the middle. The other is that the powder shape varies fairly periodically along the longitudinal axis of the magnet. This phenomenon is caused by the periodic arrangement of magnet blocks inside the magnets. It is well known that the magnetic flux density is the largest at the pole locations [15]. Hence, the periodic peak corresponds to the pole positions, whereas the periodic valley occurs at the middle of each magnetic block.

Further quantification is made from the measured thickness tabulated in Table 1 for the five magnets represented by their corresponding numerals. Magnet numbers 1 and 2 denote the magnets at the two sides whereas 2, 3, and 4 are the middle ones. It is clear that the magnets at the two sides have a larger thickness, irrespective of the X and Y directions for the reasons explained above. In addition to the shape features described above, three more features can be noticed. First,

the thicknesses in the X direction are always smaller than those in the Y direction, irrespective of the position of the magnet. Second, the thicknesses of X1 and X2 are about the same. Last, The Y2 thickness is the largest for all cases. It should be noted that a larger thickness represents a large amount of metal debris being attracted by the magnets.

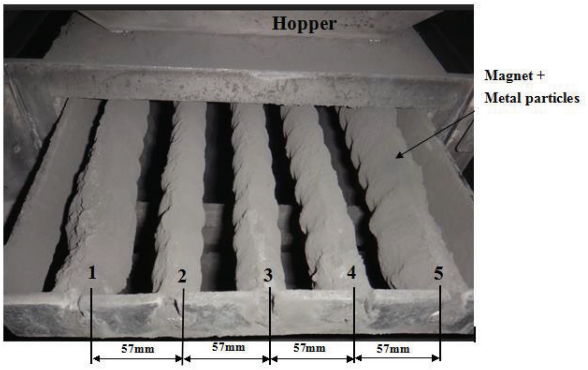


**Figure 7.** The shapes of the EMC powders attached to the magnets

**Table 1.** The thickness of EMC powders on each magnet

| Magnet No. | 1 | 2 | 3 | 4 | 5 |
|---|---|---|---|---|---|
| X1(mm) | 3.2 | 1.1 | 1.1 | 1.1 | 3.0 |
| X2(mm) | 3.2 | 1.1 | 1.1 | 1.1 | 3.0 |
| Y1(mm) | 4.3 | 1.5 | 1.5 | 1.5 | 4.3 |
| Y2(mm) | 8.0 | 6.0 | 6.0 | 6.0 | 8.0 |

As the magnetic flux density is symmetric with respect to the longitudinal axis of the magnet, the thickness distribution of the EMC powders around the magnet shows an interesting phenomenon. Apparently, debris attraction is not only influenced by the magnetic flux density but also by the flow around the magnet. For the circular magnet, the wake flow forms behind the magnet [11]. The powder velocity in the wake is smaller due to flow recirculation. In contrast, the velocity at the side of the magnet is the largest due to acceleration while that in front of the magnet is second due to flow retardation. Thus, the corresponding thickness is the smallest at the side and that in the front is slightly larger. That is, the debris removal efficiency can be enhanced by adjusting these two factors of field strength and wake recirculation.

To further understanding the accumulation rate of debris attracted by the magnets, the magnets were removed from the magnet chamber at each hour during the four hour operation period to measure the weight of the attracted metal debris. The results are shown in Fig. 8. Please note that the results shown in Fig. 5 are for the metal debris only without the covered EMC powders because the powders were dissolved by solvent already before measuring the weight of the metal debris. It can be seen that the rate of accumulation increases as the operation time proceeds. Specifically, at the first hour, the accumulation rate is 0.25g/hr; whereas at the last hour, the rate is 0.48g/hr. This situation is partly due to the van der Waals force [4] of the attracted metal debris and also due to the increased equivalent surface area of the magnet by the presence of the irregular shaped metal debris. The increased rate of accumulation also indicates that the metal debris are removed from the EMC powders effectively.

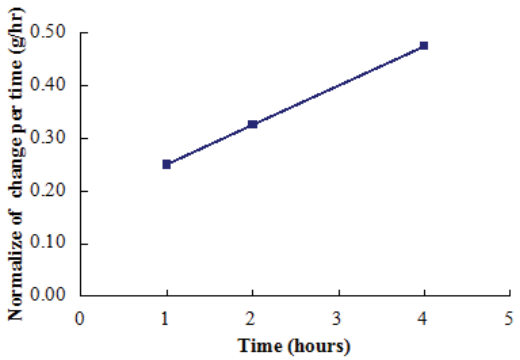


**Figure 8.** Accumulation rate of metal debris versus operation time

## 4 Conclusions

The thermosetting characteristic of current encapsulation molding compound generally leads to the generation of metal debris during its preparation. The situation is caused by the very hard silica fillers in the compound. The presence of these metal debris will cause circuit shortages and have to be removed.

In this study, Nd-Fe-B permanent magnets were used to remove these metal debris in the encapsulation molding compounds. The results show that the metal debris can be removed effectively as evidenced by the increased accumulation rate. More specifically, the metal debris removal rates are 0.25g/hr and 0.48g/hr at the first and fourth hour of the removal operation, respectively. Moreover, the backside of the magnet is the most effective region of debris removal due its recirculation flow feature.

## References

1. L. T. Nguyen, 43rd ECTC, Orlando, FL, USA, 1993.
2. S.Han and K. K. Wang, IEEE Trans. Comp., Packag., Manufact. Technol. B, **18**, 4 (1995).
3. Y. Liaw and J. H. Chou, AMR, 126-128, 2010.
4. Y. Nakai, K. Senkawa, F. Mishima, Y. Akiyama, and S. Nishijima, {IEEE} Trans. Appl. Superconduct, **21**, 3 (2011).
5. F. Mishima, T. Terada, Y. Akiyama, Y. Izumi, H. Okazaki, and S. Nishijima, {IEEE} Trans. Appl. Superconduct, **18**, 2 (2008).
6. S. Hayashi, F. Mishima, Y. Akiyama, and S. Nishijima,

IEEE Trans. Appl. Superconduct, **20**, 3 (2010).
7. Y. Nakai, F. Mishima, Y. Akiyama, and S. Nishijima, IEEE Trans. Appl. Superconduct, **20**, 3 (2010).
8. F. Mishima, S. Yamazaki, K. Yoshida, H. Nakane, S. Yoshizawa, S. Takeda, Y. Izumi, and S. Nishijima, {IEEE} Trans. Appl. Superconduct, **14**, 2 (2004).
9. D. Ruttley (Rattler Tools, Inc.) Metal debris cleanout system and method US 20060049111 A1, 2006
10. D. Ruttley (Rattler Tools, Inc.) Metal debris cleanout system and method US 7410014 B2, 2008
11. M. Van Dyke, An Album of Fluid Motion, The Parabolic Press, California, USA, 1982.
12. N. I. Kasim, M. A. Musa, H. Ngah, A. R. Razali and M. Ishak, J. EAS, **10**, 17 (2015).
13. K. Ozturk , E. Sahin , M. Abdioglu , M. Kabaer , S. Celik , E. Yanmaz , T. Kucukomeroglu, J. Alloy Compd., **643**, 201–206, 2015.
14. S. Celik, J. Alloy Compd., **662**, pp.546-556, 2016.
15. T. Dimova, M. Marinova, B. Aprahamian, 19th SIELA, Bourgas, Bulgaria, 2016.